

Molecular Structure of Azopolymers and Photoinduced 3D Orientational Order. 1. Azobenzene Polyesters

Oleg V. Yaroshchuk,^{*,†} Michel Dumont,[‡] Yuriy A. Zakrevskyy,[†] Tetyana V. Bidna,[†] and Jurgen Lindau[§]

Institute of Physics, NASU, prospect Nauki 46, 03028 Kyiv, Ukraine, Ecole Normale Supérieure de Cachan, LPQM, 61 av. President Wilson, 94235 Cachan, France, and Institute of Physical Chemistry, Martin-Luther University, Mühlphorte 1, 06108 Halle, Germany

Received: October 27, 2003; In Final Form: January 27, 2004

The combination of transmission null ellipsometry (TNE) and attenuated total reflection (ATR) methods supported by absorption measurements is shown to be an effective tool to study spontaneous and photoinduced 3D order in azopolymers. We investigated a series of azobenzene containing side-chain polyesters differing by the length of the main-chain spacer $(\text{CH}_2)_m$ ($m = 2, 8, 9, 10, 12, 13, 14, 16$) and the tail substitutes (NO_2 , OCH_3 , and OC_4H_9) in azochromophore. The 3D order was induced by monochromatic polarized light of several wavelengths strictly distinguished by absorption efficiency of azochromophores. The orientational order under irradiation and after irradiation is studied. A big variety of 3D orientations (biaxial, uniaxial, and isotropic) is realized. The uniaxial and isotropic configurations correspond to the initial state and the saturation state of irradiation, while biaxiality is an attribute of the transient orientations. It is shown that both initial and photoinduced 3D orders are strongly determined by molecular structure of azopolymers. If we exclude the case of ultrathin polymer films ($d < 200$ nm), the observed regularities can be summarized as follow. The homologues with NO_2 tail group and $m > 8$ demonstrate strong preference for in-plane alignment, which is random in the initial state and uniaxially ordered in the saturated state of irradiation. The change of the tail substitute in the succession $\text{NO}_2 \rightarrow \text{OCH}_3 \rightarrow \text{OC}_4\text{H}_9$ leads to transition from the in-plane to the out-of-plane alignment of azochromophores (nonirradiated films), increase of the tendency of isotropic ordering (excitation within $\pi\pi^*$ absorption band), and transition from the positive (prolate) to the negative (oblate) in-plane uniaxial order (excitation within $n\pi^*$ absorption band). The observed regularities are explained by competition of photoorientation determined by symmetry of light and intrinsic self-organization determined by the structure of polymer molecules.

I. Introduction

Presently, in the era of information technologies, there is an increasing interest in photonic processes allowing the improvement of devices for information storage, processing, displaying, and transfer. The phenomenon of photoinduced anisotropy (PIA) is one of the best candidates for this purpose.

Photoinduced anisotropy (also named Weigert¹ effect) produces optical dichroism and birefringence in various materials by generating an orientational order. This order is centrosymmetric (quadrupolar) and should be more correctly named *alignment*, in contrast with the *orientation* induced by poling methods (photoassisted electrical poling (PAEP)² and all-optical poling (AOP)^{3–5}), which generate a noncentrosymmetric (dipolar and octupolar) orientational order, producing nonlinear effects ($\chi^{(2)}$).

Azobenzene-containing polymers are known to be among the most effective materials for PIA generation.^{6–14} The photoinduced birefringence in some liquid crystalline (LC) azopolymers reaches 0.3. Most often, the induced order is stable, easily erasable, and rewritable. For those reasons, azopolymers present a large potentiality for practical applications.

The microscopic explanation of PIA in azopolymers is based on two properties of azochromophores:^{6,7,10} the *trans*–*cis*

reversible photoisomerization and the anisotropy of the molecular absorption, since the transition dipole moment is oriented approximately along the molecular axis. Because of these properties, two mechanisms cooperate, in proportions depending on molecular parameters and on irradiation conditions. The first mechanism is the angular selectivity of the photoexcitation, which produces *angular hole burning*. This selective depletion of the ground state is common in all photochromic materials. If photoproducts are thermally and photochemically stable, the saturation of hole burning leads to a total depletion of the initial state. The second mechanism occurs when the photochromism is thermally or optically reversible (like *trans*–*cis* photoisomerization of the majority of azobenzene derivatives). In that case, molecules undergo a great number of photoisomerization cycles resulting in a kind of mechanical stirring, which induces a random-walk rotation of azochromophores (and also a random translation well-known in relief grating experiments^{15–17}). [Note that angular redistribution seems to be also realized by vibrational excitation of molecules, but these mechanisms are less efficient and not yet well understood.] This process, known as *angular redistribution*, leads to the accumulation of molecules perpendicularly to the polarization of the exciting light. More generally, after a great numbers of photoisomerization cycles, these two processes tend to minimize the probability of optical excitation. This is also true in the case of AOP, in which the excitation is a noncentrosymmetric combination of optical

[†] NASU.

[‡] LPQM.

[§] Martin-Luther University.

fields.^{3–5} As far as molecules are in an isotropic environment, the photostationary angular distribution results from the competition between the above ordering process and the thermal diffusion in the ground state, which tends to restore the isotropy. The final symmetry of the angular distribution is then imposed by light in the hole-burning process, but the angular redistribution enhances the order and is necessary for keeping a strong anisotropy after the full relaxation of photoisomers. Let us notice that molecules are not submitted to any torque but only to a kind of Brownian motion.

When molecules are not in an isotropic environment, there is a competition between the symmetry of the photoexcitation and that of the environment. The simplest case is that of photoassisted electrical poling: the random walk of the angular redistribution occurs in the potential of an external dc field and tends to produce a noncentrosymmetric distribution along the dc field axis (there is a torque). More complicated is the case of polymers presenting an intrinsic self-organization, like liquid crystal polymers: In that case, each molecule is excited with a probability depending of its orientation with respect to the optical field, but the angular redistribution is driven by the local potential imposed by neighbor molecules. Furthermore, the change of orientation of individual molecules has a retroaction on the orientation of LC domains, which are also sensitive to the boundary conditions, particularly important in the case of thin films. In this paper we study the behavior of such materials.

A precise theoretical modelization of the photostationary state and of the dynamics of the molecular angular redistribution has been developed in the case of cigarlike molecules, submitted to an axial excitation in an isotropic polymeric environment^{18–20} (PIA with linearly or circularly polarized light, AOP with linearly polarized beams, PAEP with circularly polarized light propagating along the dc field direction). In all these cases, the uniaxiality allows a simple 2D theory, based on the decomposition of angular distributions on Legendre polynomials. In isotropic media, the generalization of this model to any kind of symmetry of the optical excitation and of the molecular structure (3D theory) is formally possible by using Wigner functions instead of Legendre polynomials, but the number of equations is too large for a practical solution of the dynamical problem. Nevertheless, with some more approximations, the photostationary state of PIA and AOP can easily be described in the most general case.²¹ In the case of LC polymer matrixes, the self-organization tendency leads to a much more difficult problem. Recently, the attempts have been made to describe the 3D photoorientation of chromophores in such materials.^{22–24}

Similarly, most of the experimental studies of photoinduced ordering of azopolymers are restricted to 2D measurements. Indeed, in these experiments, the probe beam propagates perpendicularly to the plane of the studied film so that only the two in-plane components of the real, or the imaginary, part of the index of refraction can be measured. When the material is isotropic and when the excitation is uniaxial (linear polarization), one can assume that the third direction is equivalent to one of the two directions experimentally measured. In this case results of 2D measurements allow us to predict 3D orientational distribution.^{10,25} However, often these conditions are not fulfilled, particularly when the self-organization of materials produces unpredictable 3D order. Some authors^{12,26} deduce the absorption coefficient in the direction of the normal to the film from the variations of the absorption for the two in-plane main axes. This is valid if the 3D order is known before photoexcitation (or at any instant of time t_0) and if the probe beam is not affected by the excitation of chromophores to higher excited

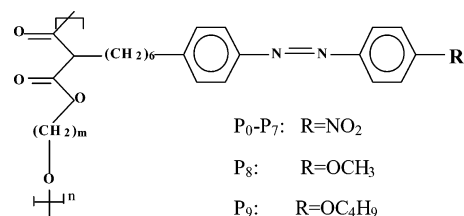


Figure 1. Structure of the azopolymers studied in this paper.

states so that the sum of the three absorption coefficients is constant. This means that the probe wavelength must be in a spectral range that is not affected by the photochromism (in refs 12 and 26 the authors use IR vibrational transitions) or that measurements must be done after full relaxation of excited states.

Unfortunately, the approaches described above may be applied only in some particular cases. In general case, the determination of the 3D orientational distribution needs the measurement of the birefringence or the dichroism for different incidence angles of the probe beam. In this paper, we use two experimental methods based on this idea: the *attenuated total reflection* method (ATR), which has been widely used for the study of PIA and PAEP in isotropic azopolymers,^{10,27,28} and the *transmission null ellipsometry* method (TNE), adapted for the study of PIA in isotropic and LC polymers.^{23,24,29–31} Both methods will be described in subsection C (section II).

In the past decade, several groups have been studied the influence of the molecular architecture on the PIA characteristics. Kulinna et al.³² investigated photoordering processes in a series of 4-cyanoazobenzene side-chain polyesters, varying the length of alkyl spacers in the side and the main polymer chains. Brown et al.³³ studied the variation of PIA properties in a series of 4-nitroazobenzene poly(methyl methacrylate)s with various concentrations of the azobenzene moieties. Recently, Wu et al.³⁴ reported peculiarities of photoorientation in a series of polymethacrylate copolymers containing 4-ethylazobenzene and cyanobiphenyl side chains. These studies revealed the essential influence of molecular structures on the kinetics, magnitude, and stability of the induced orientational order. However, in these studies, the 3D character of the orientation was not considered and a simple uniaxial order was postulated.

In this research we investigate the influence of the molecular architecture on the 3D configuration of azochromophores. For this purpose, we use a series of polyesters with azochromophore side chains. The structure of main chains, as well as the structure of azochromophores, is varied. We try to show how modification of various polymer fragments influences the 3D orientation of azochromophores in nonirradiated and irradiated films. These empirical rules should help to design polymers with desirable parameters for PIA.

II. Experimental Section

A. Polymer Synthesis and Characterization. We used a series of polymalonates differing by the main-chain alkyl spacers and by the end substitutes of the side-chain azochromophore. Figure 1 shows the general formula of these compounds, and Table 1 gives the number of spacers and the tail substitute for each symbolic name. The synthesis of polyesters was carried out as described previously.³⁵ It was based on the polycondensation of mesogenic diethylmalonates with appropriate diols. The synthesized polyesters were characterized by elemental analysis and ¹H NMR spectroscopy. The results are in agreement with the proposed structures. Molecular weights of polymers

TABLE 1: Characteristics of Polymers Studied in This Paper^a

polymer	m	R	transitn temps, °C	M_n , g/mol	$\pi\pi^*$ abs max, nm
P ₀	2	NO ₂	C 60 S 134 I	2600	348
P ₁	8	NO ₂	C ₁ 32 C ₂ 44 S 52 N 55 I	7000	391
P ₂	9	NO ₂	C (G5 S 47N 55 I) 45 N 55 I	20700	379
P ₃	10	NO ₂	C (N 51 I) 53 I	12800	383
P ₄	12	NO ₂	C ₁ (N 52 I) 68 C ₂ 76 I	21800	363
P ₅	13	NO ₂	C (G 20 N 56 I) 46 N 56 I	8600	359
P ₆	14	NO ₂	C (N 55 I) 57 I	9300	357
P ₇	16	NO ₂	C 73 I	16600	354
P ₈	8	OCH ₃	G 7 C 58 N 62 I	7519	360
P ₉	8	OC ₄ H ₉	C 63 N 75 I	5820	318

^a *m* refers to the number of main chain spacers, and R is the tail radical of azochromophores, as shown in Figure 1.

were determined by gel permeation chromatography. The data for number-average molar mass M_n are presented in Table 1.

The phase transitions were studied by polarization microscopy and differential scanning calorimetry (DSC). From these studies, LC properties were revealed in all homologues, except P7. The phase transition temperatures, presented in Table 1, refer to bulk polymers. Symbols C, C₁, and C₂ correspond to crystalline phases, G corresponds to glassy states, S and N correspond to smectic and nematic mesophases, respectively, and I corresponds to isotropic melts. Temperatures in parentheses correspond to the second heating, after a first heating and a subsequent cooling. As one can see, these polymers have a propensity for crystallization, which is a quite common behavior for side-chain polyesters.^{32,36} At room temperature our polymers are more likely to be in a semicrystalline phase. This is confirmed by the observation of both glassy and crystal melting peaks on DSC records of P2, P5, and P8.

B. Film Preparation. Polymer films were prepared by spin coating of polymer solutions in dichloroethane (2 wt %). For spectral and ellipsometry studies, the films were cast on quartz slides, while those for the ATR measurements were cast on glass slabs previously coated with a semitransparent gold layer. The spin velocity was varied to change a thickness of the films. The thickness of each film was evaluated with a profilometer. In the case of ATR studies the film thickness *d* was adjusted to 1–2 μm, which is optimal for this method. The films were backed at 40 °C over 8 h to complete solvent evaporation.

The optical quality of films strongly depends on their thickness. As a rule, thin films (*d* < 0.5 μm) are uniform and have good optical properties. Thicker films are often turbid, probably because of partial crystallization. The typical microscopic textures of thin and thick films are shown in Figure 2. It is evident that the thin film has a homogeneous structure, whereas the thick film exhibits grains, which are presumably microcrystallites. This classification is rather conditional, since the homogeneous structure can be changed into grained one by heating above *T_c* and by cooling rapidly to room temperature. Moreover, thick films can be obtained as homogeneous by either slow evaporation of the solvent or slow cooling from isotropic phase. This conclusion is in full agreement with results of calorimetric studies. In addition, homogeneous structures are more stable in thin films because of polymer interaction with the solid substrate.

C. Methods. The photoordering processes were initiated by irradiation with polarized light directed normally to the films. Three different wavelengths were used to pump the samples:

(1) $\lambda_{\text{ex1}} = 365$ nm, from a mercury lamp, selected by an interference filter and polarized with a Glan prism. The light intensity *I* was varied in the range 4–80 mW/cm².

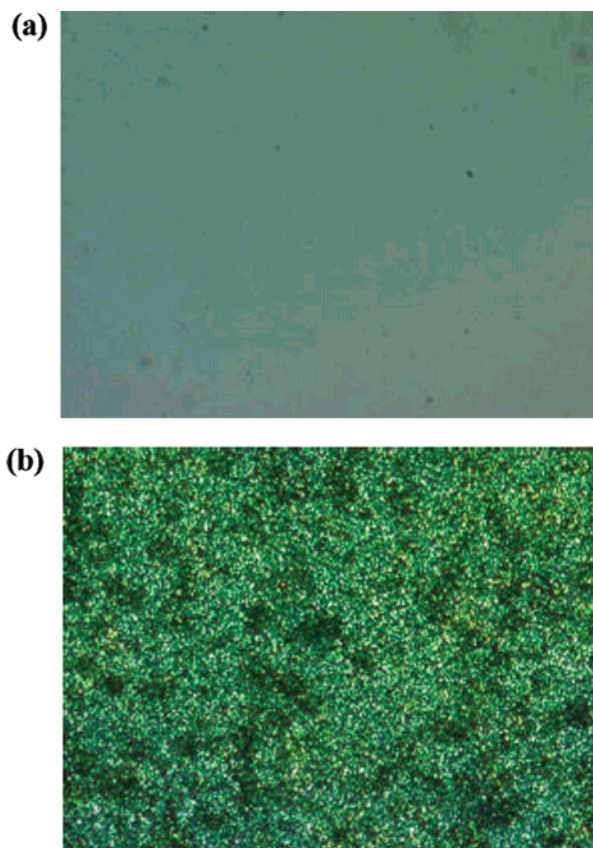


Figure 2. Optical textures of P1 films at room temperature. Textures a and b correspond to the film thickness 120 and 1100 nm, respectively. The angle between polarizer and analyzer is (a) 80° and (b) 90°. The magnification is ×400.

(2) $\lambda_{\text{ex2}} = 457$ nm from an Ar⁺ laser (*I* ≤ 200 mW/cm²).

(3) $\lambda_{\text{ex3}} = 488$ nm from an Ar⁺ laser (*I* ≤ 800 mW/cm²).

As will be shown below, the line $\lambda_{\text{ex1}} = 365$ nm corresponds to strong absorption of azochromophores, whereas the lines $\lambda_{\text{ex2}} = 457$ nm and $\lambda_{\text{ex3}} = 488$ nm lie on the wing of the UV/visible absorption band. In all cases the polarization of light was chosen, by definition, along the *x* axis of the Cartesian coordinate system with *x* and *y* axis parallel to the verges of the rectangular polymer film and *z* axis normal to this film.

Analyzing various experimental approaches, we concluded that the most reliable methods for the study of 3D orientational order in azopolymers are the methods giving directly the three components of the index of refraction. To determine azochromophore distribution, we assume that the direction (directions) of the maximum refractive index corresponds to the direction (directions) of the maximum of the angular distribution of azochromophores. This implies that the probe wavelength lies on the red wing of the main absorption band of chromophores, where the associated dispersion is strong and positive. Near-IR and, frequently, red light are suitable for these measurements. 2D absorption methods, particularly UV/visible and IR spectroscopy, give valuable preliminary information for estimating the order parameters of azochromophores and of other molecular fragments.^{12,26,37}

In these studies two methods dealing with refractive indices have been adapted to azopolymers. One of them is *attenuated total reflection* (ATR) used in the Kretschman configuration. This method has been widely described in previous publications.^{10,19,27} A glass slide, with an evaporated semitransparent gold layer, is spin-coated with the polymer film and is put in optical contact with the flat surface of half-sphere having the

same index of refraction. An IR laser beam (laser diode at 830 nm) is reflected on the sample, through the half-sphere, and the reflectivity is measured as a function of the incidence angle, with a computer-driven goniometer. The angular positions of the Fabry–Perot dips, for both TE and TM polarizations, give three principal components of the refractive index, n_x , n_y , and n_z and the thickness of films, d . The method provides precision of n_x , n_y , and n_z of the order of 0.01. These measurements were carried out for the polymer films before and after irradiation, as well as in a stationary state of irradiation ($\lambda_{\text{ex1}} = 365$ nm and $\lambda_{\text{ex2}} = 457$ nm). The ATR method was applied to study P1, as representative of P1–P7 polymers with quite similar photoorientation characteristics, as well as P8 and P9.

The second method is the *transmission null ellipsometry* (TNE),^{23,24,29} which is based on the Senarmont method. The probe beam (628 nm) is linearly polarized at 45° with respect to the in-plane main axes of the sample. The elliptically polarized transmitted beam is converted into a linearly polarized beam by a quarter wave plate (axis parallel to that of the polarizer). The angle φ of the output polarization, determined by rotation of a linear analyzer, gives the in-plane retardation $(n_y - n_x)d$. Then the sample is rotated around the x axis vertically aligned and the polarization angle φ is measured as a function of the incidence angle θ . The out of plane retardation $(n_z - n_x)d$ is determined by fitting a theoretical expression of $\varphi(\theta)$. The TNE was used to study 3D orientation of azochromophores in all polymers, before irradiation and after successive irradiation steps with $\lambda_{\text{ex1}} = 365$ nm and $\lambda_{\text{ex3}} = 488$ nm exciting light.

Each of these two methods has some advantages and disadvantages. The indisputable advantage of ATR method is direct estimation of principal refractive indices. On the basis of these data and the symmetry of pumping light, the spatial configuration of azochromophores can be easily found. The ATR method permits one to determine the 3D orientation in the photostationary state as well as to monitor transient reorientations. The transient of refractive indices under irradiation identifies the tendency of the photoreorientation of azochromophores without any additional measurements. The drawback of this method is that it requires an excellent optical quality of films and the optimization of films thickness. The first demand is difficult to satisfy for LC azopolymers, because of their domain structure,³⁸ whereas the second one complicates investigation of films having nonoptimized thickness. For these reasons, films for ATR studies should be thoroughly selected.

In contrast to ATR, the demands of transmission ellipsometry for the optical quality of films are not so strong. The method can be applied to films of various thicknesses, which allows us to study the influence of films thickness on the orientational configuration. The film can be removed from the setup between two successive measuring steps, to carry out additional tests (absorption measurements, microscopic observation, etc.). Nevertheless, to determine unambiguously the preferential photoorientation directions of azochromophores, the TNE method requires additional investigations (as a rule, measurement of at least one principal refractive index before irradiation). Moreover, our TNE set up is not adapted to study orientation under irradiation.

Thus, ATR and TNE methods supplement each other. Furthermore, in many cases, results obtained with these methods can be compared. This gives a chance to check the reliability of both methods and the trustworthiness of the obtained results.

As a complementary characterization method, we also perform 2D dichroism measurement in the UV/visible spectral range. The optical densities, D_x and D_y , corresponding to x and

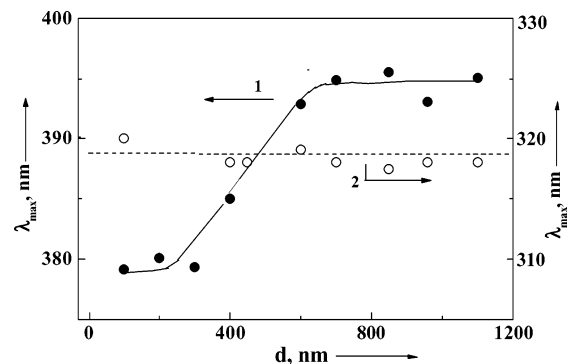


Figure 3. Wavelength of the maximum of the $\pi\pi^*$ absorption band versus film thickness: (1) for P1; (2) for P9.

y in plane polarizations, are measured with a probe beam propagating perpendicularly to the sample. The third component, D_z , is estimated by the *total absorption method*, which presumes the conservation of the total absorption $D_{\text{tot}} = D_x + D_y + D_z$. This conservation is valid, if the probe wavelength is sensitive only to the orientation of molecules, but not to the photochromism,^{12,26} and/or if the measurement is done after the full relaxation of the excited states of molecules (relaxation of cis, back to trans, for the $\pi\pi^*$ absorption band of azochromophores).^{23,24,37} D_{tot} can be estimated, if the 3D anisotropy is known at some instant of time t_0 . The problem is easy, if at t_0 the sample is uniaxial, with an in-plane orientation of the axis of anisotropy, e.g. y . Then

$$D_{\text{total}} \equiv D_x(t_0) + D_y(t_0) + D_z(t_0) = 2D_x(t_0) + D_y(t_0) \quad (1)$$

If the number of azobenzene units in trans configuration remains constant at each instant of time t , D_z can be estimated as

$$D_z(t) = D_{\text{total}} - D_x(t) - D_y(t) \quad (2)$$

where $D_x(t)$ and $D_y(t)$ are experimentally measured. Then, the diagonal terms of the tensor of orientational order S_{ij} can be estimated. For example

$$S_{xx} = \frac{D_x - \frac{1}{2}(D_y + D_z)}{D_x + D_y + D_z} \quad (3)$$

The components S_{yy} and S_{zz} can be obtained by cyclic permutation in expression (3). In the case of axial symmetry, for instance around y , one defines the order parameter S :

$$S \equiv S_{yy} = -2S_{xx} = -2S_{zz} \quad (4)$$

The total absorption method can be applied in some experimental situations described below.

The UV/vis absorption measurements were carried out using a S2000 diode array spectrometer from Ocean Optics Co. The samples were set normally to the testing light from a low-intensity deuterium lamp. A Glan-Thomson prism was used to polarize the probe beam.

III. Results and Discussion

A. Photochemical Properties. 1. UV/Vis Spectra of Non-irradiated Films. First UV/visible spectra for films of various thicknesses have been measured. For polymers P1–P7, we found considerable changes of the position of the most intense absorption band, $\pi\pi^*$ band, with the variations of the films thickness d . The curve 1 in Figure 3 shows that the wavelength

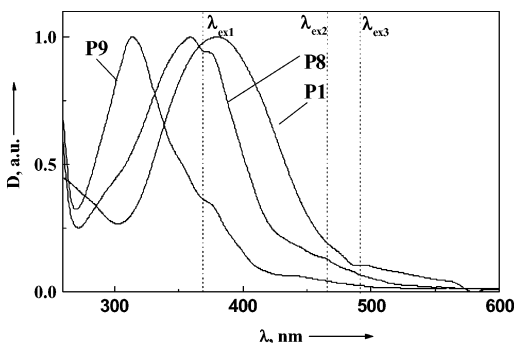


Figure 4. UV/vis unpolarized spectra of the films of P1, P8, and P9 polymers.

of the $\pi\pi^*$ absorption maximum, λ_{\max} , of P1 gradually increases with the thickness and reaches constant value above $d = 600$ nm. This tendency is also observed for polymers P2–P7; however, the variation generally weakens with the increase of m . Despite the same structure of azochromophore, the thickness effect is not observed for P0. The $\lambda_{\max}(d)$ dependence for P9 is presented in Figure 3 with curve 2. It does not show any substantial dependence of λ_{\max} on the film thickness. Similar behavior is also observed for P8 films. Thus variation of λ_{\max} is not essential for homologues containing chromophores with alkyl substitutes.

In P1–P7 homologues, the film thickness effect makes a challenge in the comparison of spectra of various polymers. Only spectra of relatively thick films, with stable value of $\lambda_{\max}(d)$, can be compared. On the other hand, thin films are preferred, to minimize formation of grains, which causes light scattering and deformation of the spectrum. The compromise was found for the film thickness in the range 0.6–1.5 μm . Fortunately, this range overlaps with the thickness range required for ATR method. For all these reasons, in these studies, we used only films with optimized thickness, i.e., with $d = 0.6$ –1.5 μm . During coating of these films, evaporation rate of solvent was reduced, to avoid nucleation and the resulting light scattering.

Figure 4 shows nonpolarized UV/visible spectra of some homologues. Each spectrum contains a strong $\pi\pi^*$ absorption band, while the weak $n\pi^*$ bands cannot be clearly identified. The wavelength of the maximum of the $\pi\pi^*$ absorption band, λ_{\max} , is presented in Table 1, for all homologues. In a comparison of the values of λ_{\max} , the following conclusions can be drawn:

(1) λ_{\max} increases in the order $\text{OC}_4\text{H}_9 \rightarrow \text{OCH}_3 \rightarrow \text{NO}_2$.

(2) The general tendency for the polymer series P1–P7 is a gradual decrease of λ_{\max} with the increase of m . P0 appears as an exception, for which λ_{\max} demonstrates strong hypsochromic shift, compared with neighbors P1 and P2.

The first conclusion is evident, since λ_{\max} is maximally shifted to the red for chromophores with pronounced donor–acceptor properties. The second conclusion may be explained assuming H-aggregation of azochromophores.³⁹ In fact, the aggregation should be essential in homologues with NO_2 substitutes, which are strongly polarized because of the push–pull effect. The aggregation rate should be especially high for homologues having high content of chromophores. This can explain strong hypsochromic shift of λ_{\max} in case of P0. On the other hand, the gradual hypsochromic shift of λ_{\max} in the succession $m = 8, 9, 10, 12, 13, 14,$ and 16 may be caused by the enhancement of the mobility of azochromophores leading to their segregation and effective formation of H-aggregates. So, the homologues with the intermediate m ($m = 8$ –12) seem to be the less aggregated. The pronounced decrease of λ_{\max} , with decreasing

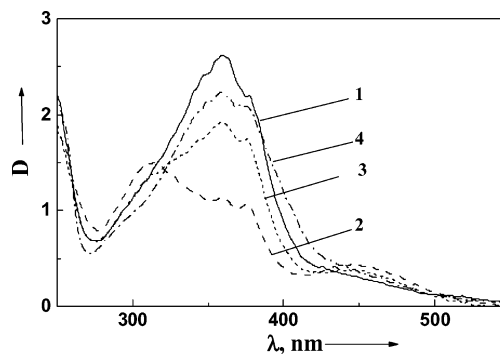


Figure 5. UV/vis spectra of a P8 film: (1) before irradiation; (2) after irradiation with $\lambda_{\text{ex1}} = 365$ nm and $I = 25$ mW/cm^2 for 30 min; (3) 30 min relaxation of spectrum 2; (4) irradiation with $\lambda_{\text{ex1}} = 365$ nm and $I = 25$ mW/cm^2 for 30 min and, subsequently, with $\lambda_{\text{ex3}} = 488$ nm and $I = 750$ mW/cm^2 for 5 min.

the film thickness, may be also explained by the enhancement of H-aggregation of azochromophores at the polymer–substrate interface, presumably due to self-assembling processes.⁴⁰

2. UV/Visible Spectra of Irradiated Films. The wavelengths of excitation light are shown in Figure 4 by dotted vertical lines. One can see that $\lambda_{\text{ex1}} = 365$ nm line falls into the central part of $\pi\pi^*$ absorption bands, i.e., in the spectral range of the absorption maximum. In contrast, $\lambda_{\text{ex2}} = 457$ nm and $\lambda_{\text{ex3}} = 488$ nm lines correspond to the red wing of $\pi\pi^*$ absorption bands and the presumed weak $n\pi^*$ absorption bands.

With each of these three excitation lines, the spectra of P0–P7 polymers before and after irradiation (after 10 min relaxation) are practically identical. The spectral changes corresponding to trans–cis isomerization were detected only under irradiation. This shows that the lifetime of cis isomers is short (of the order of seconds or tens of seconds). [Note that the problem of the measurement of the lifetime of cis isomers is expounded in ref 24.]

The spectra of P8 polymer for different irradiation doses are shown in Figure 5. The spectral changes observed for $\lambda_{\text{ex1}} = 365$ nm irradiation correspond to classical trans–cis photoisomerization (decrease of the main $\pi\pi^*$ absorption band and growing of weak $n\pi^*$ band on the red wing of the spectrum). For low irradiation doses, the relaxation kinetic can be roughly described by an exponential function, with a characteristic time of 15 min, which is assigned to the lifetime of thermal relaxation of cis isomers. For high irradiation doses, there is also increasing fraction of long-living photoisomers (lifetime of about 1 h). Figure 5 shows that sample can be transferred back to the initial trans state by irradiation with $\lambda_{\text{ex3}} = 488$ nm, which lies in the $n\pi^*$ absorption band of cis form. By direct irradiation with only $\lambda_{\text{ex3}} = 488$ nm, trans–cis isomerization was not detected. Indeed, at this wavelength, the excitation rate from trans to cis is much less than that from cis to trans and the photostationary state corresponds to a negligibly small population in cis form. Nevertheless, a variation of the optical density is observed, without change of the spectral shape, which might correspond to the reorientation of trans isomers. This also proves that isomerization cycles are efficient although not observable directly.

The spectra obtained for irradiated P9 films are presented in Figure 6. The photochemistry of this polymer is more complicated than that of other homologues in the studied series. In parallel with the changes typical for trans–cis isomerization (decrease of the $\pi\pi^*$ band at 320 nm and increase of the $n\pi^*$ band at 450 nm), the $\lambda_{\text{ex1}} = 365$ nm irradiation leads to the appearance of a new absorption band with a maximum at 360

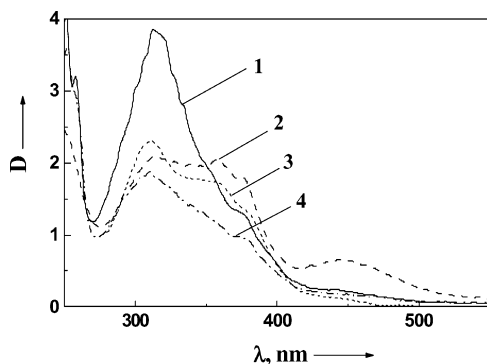


Figure 6. UV/vis spectra of P9 film: (1) before irradiation; (2) after irradiation with $\lambda_{\text{ex1}} = 365$ nm and $I = 25$ mW/cm² for 30 min; (3) 3 h relaxation of spectrum 2; (4) irradiation with $\lambda_{\text{ex1}} = 365$ nm and $I = 25$ mW/cm² for 30 min and, subsequently, with $\lambda_{\text{ex3}} = 488$ nm and $I = 750$ mW/cm² for 5 min.

nm. This band seems to be caused by some unknown photochemical product. Both reactions are slowly reversible. The relaxation time of cis isomers, estimated by the relaxation of the $n\pi^*$ band, is of the order of 2.5 h, whereas the lifetime of the other photoproduct, estimated by the relaxation of the 360 nm band, is about 9 h. The 488 nm irradiation of P9 films, preliminarily pumped with 365 nm light, leads to the complete erasure of the 360 and 450 bands, but the $\pi\pi^*$ band never returns to its initial level. The direct irradiation with only 488 nm did not cause spectral shape modifications typical for trans-cis isomerization but some reduction of absorption, which might be assigned to reorientation and, possibly, degradation of azochromophores at high irradiation doses.

On the basis of the photochemical results, one can make some predictions regarding photoordering mechanisms. Since trans-cis isomerization is the only detectable photoreaction in polymers with push-pull chromophores (P0–P7) and since the lifetime of cis isomers is only several seconds, one can predict that photoreorientation mechanism dominates for any type of irradiation. In P8 with the long-living cis isomers (lifetime is more than 15 min) and in P9 with almost stable photoproducts (lifetimes are 2.5 and 9 h) the reorientation will be difficult and will depend on the wavelength of excitation. If the pumping back of the photoproducts is not efficient, the photoselection (angular hole burning) mechanism of PIA with a depletion of the trans state will dominate.

One more important conclusion relates to methodology of measurements. Since the lifetime of cis chromophores in P1–P7 polymers is of the order of seconds, the concentration of trans isomers is practically the same before irradiation and 1 min after successive irradiation steps. This proves validity of total absorption method for P1–P7 homologues. The time gap between irradiation and all measurements was chosen as 15 min, i.e., longer than 1 min, to reach both relaxation of cis isomers and stabilization of the induced order, which usually enhances in these polymers after irradiation.¹⁴ The same time gap is used for P8 and P9 polymers. In the case of P8 it corresponds to the major time of photochemical relaxation. In the case of P9, this time gap is short compared with the relaxation time of photoproducts and so, roughly, the nonrelaxed orientational distribution is measured. For 365 nm irradiation the total absorption method cannot be applied to P8 and P9 polymers, because of generation of the long-living photoproducts. At the same time, this method could be applied in the case of 488 nm irradiation of P8, because of low concentration of cis isomers in the irradiated films.

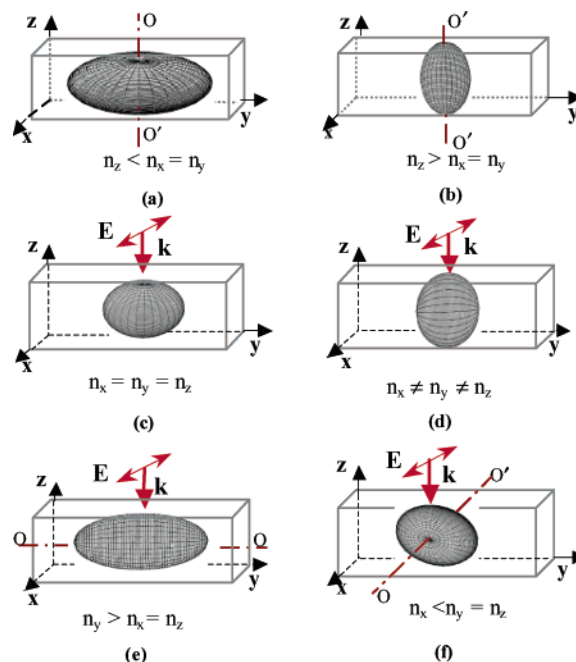


Figure 7. Different kinds of 3D orientational distributions of azochromophores: (a) negative (oblate) ordering with respect to the film normal (optical equivalent of a negative C crystal plate); (b) positive (prolate) ordering with respect to the film normal (optical equivalent of a positive C crystal plate); (c) spatial isotropic distribution; (d) biaxial orientational distribution; (e) positive ordering with respect to the in-plane axis perpendicular to the exciting light polarization (optical equivalent of a positive A crystal plate); (f) negative ordering with respect to the in-plane axis parallel to the exciting light polarization (optical equivalent of a negative A crystal plate).

B. 3D Order in the Nonirradiated Films. In this section, we mostly refer to the results of TNE studies, since results of ATR method for nonirradiated films are not always reliable. For these films, commonly, TM modes are very broad, while TE modes are not clear that complicated fitting procedure. The reason for this is not sufficiently good optical quality of the films of LC polymers for ATR measurements. The ATR results we refer to are obtained for exclusive films thoroughly selected.

The results of TNE show that preferential 3D orientation depends both on the structure of chromophores and on the length of main-chain spacers. The NO₂-tailed chromophores in all polymers, except P0, strongly prefer in-plane random alignment (Figure 7a). This alignment is characterized by an axial symmetry with respect to the normal z , with an oblate orientational distribution characterized by a negative order parameter. Films with this type of alignment are optically equivalent to negative C crystal plates. The strong preference of azochromophores in polymer P1 for in-plane alignment is confirmed by ATR measurements (Table 2).

In P0, which has a short main-chain spacer, the azochromophores have preference for out-of-plane (homeotropic) alignment, as depicted in Figure 7b. This is an uniaxial alignment in the direction of the film normal z (prolate orientational distribution), with a positive order parameter. Such films, with a homeotropic order, have optical properties of positive C crystal plate.

Random in-plane and slight homeotropic alignments are typical respectively for P8 and P9 polymers. In contrast to P1, for which results are well reproducible, for P8 and P9 we can discuss only tendency. Particularly, in some P9 films homeotropic alignment is very weak and the films can be considered as quasi-isotropic (Figure 7c). Besides, some P8 and P9 films

TABLE 2: ATR Results for P1 Films Corresponding to 365 and 457 nm Irradiation^a

film	film history	film params					film struct
		$d, \mu\text{m}$	n_x	n_y	n_z	$\langle n \rangle$	
P1-1	before irradiatn	Irradiation with $\lambda = 365 \text{ nm}$ (x Polarization, 50 mW/cm^2)					negative C film
	under irradiatn, 35 min	1.344	1.616	1.615	1.551	1.594	positive A film
	relaxatn, 60 min	1.364	1.578	1.607	1.566	1.584	positive A film
P1-2	before irradiatn	Irradiation with $\lambda = 365 \text{ nm}$ (x Polarization, 80 mW/cm^2)					negative C film
	under irradiatn, 25 min	1.348	1.577	1.584	1.577	1.579	isotropic film
	relaxatn, 50 min	1.339	1.562	1.625	1.552	1.580	positive A film
P1-3	before irradiatn	Irradiation with $\lambda = 457 \text{ nm}$ (x Polarization, 80 mW/cm^2)					negative C film
	under irradiatn, 30 min	1.363	1.610	1.596	1.557	1.587	positive A film
	relaxatn, 40 min	1.377	1.551	1.610	1.566	1.576	positive A film
		1.363	1.559	1.624	1.565	1.584	positive A film

^a n_x , n_y , and n_z are principal refractive indices; $\langle n \rangle = (n_x + n_y + n_z)/3$.

possess local biaxiality with pronounced in-plane order, which seems to be influenced by spin coating procedure.

To summarize, the following regularities were established:

(1) Lengthening the alkyl spacers in the main polymer chain leads to stronger in plane alignment of push-pull azochromophores.

(2) The change of the tail substitute of chromophores in the succession $\text{NO}_2 \rightarrow \text{OCH}_3 \rightarrow \text{OC}_4\text{H}_9$ enhances tendency of the out-of-plane alignment of chromophores.

It is difficult to explain the observed rules at the microscopic level, since the macroscopic orientation is the result of interactions between different polymer fragments as well as between the fragments and substrate. Nevertheless, these empirical regularities allow us to predict alignment tendency of azochromophores in other polymers.

C. 3D Order in the Irradiated Films. 1. *Irradiation with Polarized UV Light ($\lambda_{\text{exl}} = 365 \text{ nm}$).* The irradiation procedure substantially improves optical quality of the polymer films, as a consequence of the melting of crystallites. In ATR experiments, TE modes become apparent, while TM modes considerably narrow. Consequently, the obtained results are more reliable and reproducible. Usually, 1 day after irradiation, the films return to the multidomain state that complicates study of the relaxation properties.

First we consider polymers containing push-pull chromophores (P0–P7). The significant photoinduced changes of the birefringence were detected in all polymers of this series, except P0, for which the modifications of birefringence are strongly restricted by the aggregation of azochromophores. Apparently, the H-aggregates should be effectively destroyed to switch on the photoorientation mechanism. This seems to be not achieved in P0, for the UV intensities used in our experiments.

The values of the in-plane, $(n_y - n_x)d$, and the out-of-plane, $(n_z - n_x)d$, retardation of P1 film are presented in Figure 8a. The data correspond to successive exposure doses (x polarization of UV irradiation). The time gap between irradiation and measuring steps, for this and other polymers, was about 15 min. On the first irradiation steps, $n_y > n_x > n_z$, which correspond to a biaxial order (Figure 7d). On the following steps, the experimental curves saturate: one obtains $n_y > n_x = n_z$, which expresses uniaxial prolate distribution of azochromophores with the ordering axis parallel to y , the in-plane axis perpendicular to light polarization. Optically this film is equivalent to a positive A crystal plate (Figure 7e).

In parallel with birefringence measurements, the in-plane optical densities, D_x and D_y , of P1 films have been measured. These results are presented in Figure 9a. The kinetics of D_x and D_y can be assigned to reorientation mechanism, since

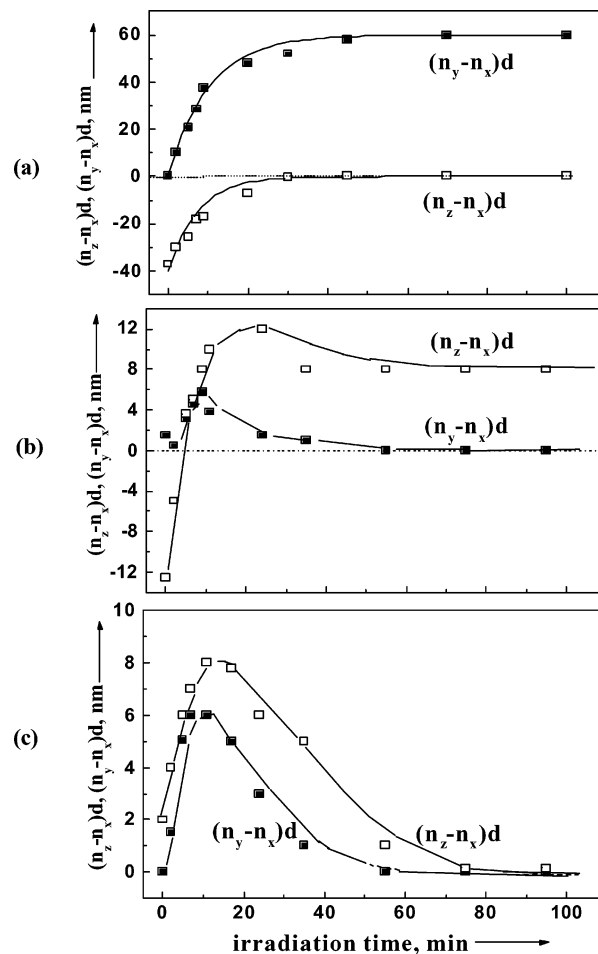


Figure 8. Birefringence kinetics for polymers (a) P1, (b) P8, and (c) P9 for successive exposure doses. Irradiation is with $\lambda_{\text{exl}} = 365 \text{ nm}$ ($I = 4.5 \text{ mW/cm}^2$, x polarization).

measurements are made after full relaxation of the cis isomers. For the same reason, the D_z component can be calculated by using the total absorption method. The normalization (time t_0 , in expression (1)) is made at saturation of $D_{x,y}(t)$ curves by setting $D_z = D_x$, since the sample becomes uniaxial in this state. The values of D_x , D_y , and D_z are used to calculate order parameters as described in subsection C (section II). The results are presented in Figure 9b. Before irradiation, $S \equiv S_{zz} = -0.07$ and $S_{xx} = S_{yy} = -S_{zz}/2 = 0.035$ (negative (oblate) uniaxial order along z). In the first steps of irradiation, S_{xx} , S_{yy} , and S_{zz} are different because of a biaxial order. At saturation $S \equiv S_{yy} = 0.25$ and $S_{xx} = S_{zz} = -S_{yy}/2 = -0.125$ (uniaxial positive order

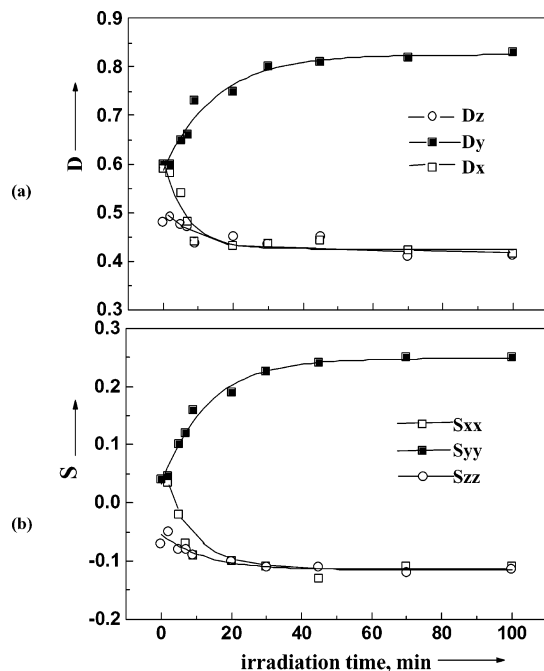


Figure 9. Kinetics of (a) D_x , D_y , D_z and (b) S_{xx} , S_{yy} , S_{zz} for successive exposure doses (polymer P1). Irradiation conditions are the same as in Figure 8.

along y). Note that absolute values of S are poorly reproducible for different films; the reproducibility is about 20% for the irradiated films and reaches 50% for the nonirradiated samples. This seems to be mainly caused by the difference in film thickness and coating conditions.

The 3D orientation under irradiation (in the photostationary state) and, subsequently, after switching off the exciting light was also studied by the ATR method. The data obtained for polymer P1 are summarized in Table 2. First, one can conclude that ATR results corresponding to 1-h relaxation are in good agreement with the asymptotic results obtained by TNE; both of them show uniaxial in plane ordering of azochromophores. This is reasonable, since in both experiments the total irradiation dose corresponds to saturation of the photoinduced order.

Under irradiation, when the photostationary equilibrium is reached, the observed structure depends on the irradiation intensity. The uniaxial in-plane orientation is observed when $I < 50$ mW/cm² but with an orientational order poorer than after irradiation. The higher is the pumping intensity, the lower is the orientational order under irradiation. For $I > 80$ mW/cm², the film becomes isotropic. This isotropic state seems to be due to the high concentration of nonmesogenic *cis* isomers. Indeed, it is well-known that *cis* isomers influence phase transitions and even suppress liquid crystalline properties in LC azopolymers, similarly to ordinary LC.⁴¹ A more interesting phenomenon is the restoration of a strong orientational order, after switching off the irradiation, even when the film was isotropic under irradiation. The 2D analogue of this effect was earlier described in ref 14. It implies a strong mesogenic effect and some orientational memory, more likely to be caused by ordering of the polymer matrix, which may persist even when the order of azochromophores is destroyed. This behavior is quite different from that of isotropic polymers (like PMMA-DR1¹⁰), in which anisotropy is reduced by saturation at high pumping intensity, but is not restored after irradiation.

Qualitatively, the results obtained for other polymers from P1–P7 series are similar: films are biaxial during the initial irradiation stage and uniaxial at saturation. In the process of

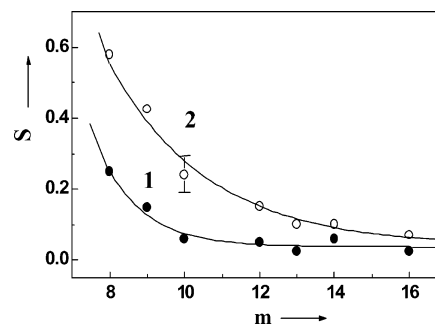


Figure 10. Order parameter $S = S_{yy}$ at saturation of irradiation, versus the number m of CH₂ groups in a spacer (Figure 1), for polymers P1–P7: (1) $\lambda_{ex1} = 365$ nm ($I = 4.5$ mW/cm²); (2) $\lambda_{ex3} = 488$ nm ($I = 750$ mW/cm²).

irradiation, chromophores reorient preferentially in plane of the film, perpendicularly to the light polarization. This kind of reorientation reminds one of in-plane switching of nematic liquid crystals.⁴² The values of the scalar order parameter at saturation, versus the number of CH₂ groups in the main-chain spacer, are shown in Figure 10 (curve 1). One can see that the order parameter monotonically decreases with increasing the spacer length. Comparing these results with results of DSC studies, one can conclude that the photoinduced order in polymers having both smectic and nematic phases (P1 and P2) is higher than that of homologues with only a nematic phase (P3–P6). This corresponds to a regularity earlier observed for the thermodynamic orientational order of low-molecular-weight liquid crystalline compounds.⁴³ One can also conclude that photoinduced order in homologues having LC phases is substantially higher than in P7, which does not have any LC phase. This is in full agreement with observations of many other authors.^{11,32}

The observed similarities between LC azopolymers and low-molecular-weight LC allow us to assume that, through activation of the molecular mobility, the irradiation stimulates self-ordering processes intrinsic for the liquid crystalline compounds. Reciprocally, this intrinsic ordering tendency enhances the orientational order caused by the photoreorientation of azochromophores. Nevertheless, it is not correct to build full analogy between thermodynamically stable spontaneous order in liquid crystals and metastable photoinduced order, “frozen” in the polymer matrix of LC azopolymers. The evidence for it is the small value of order parameters of photoinduced orientation ($\lambda_{ex1} = 365$ nm), in comparison with the order parameter of LC. Thus, these results suggest only partial influence of the intrinsic self-ordering on the formation of 3D orientation under irradiation.

Figure 8b shows the variations of $(n_y - n_x)d$ and $(n_z - n_x)d$ versus the irradiation time for polymer P8. As can be seen, before irradiation, the film is slightly biaxial with a strong preference for in-plane alignment of azochromophores ($n_z < n_x \leq n_y$). In the process of irradiation, the out of plane phase retardation $(n_z - n_x)d$ changes the sign and saturates, with $n_z > n_x = n_y$. The in plane retardation changes nonmonotonically: it reaches maximum and then decreases to 0. In the saturation state, azobenzene chromophores are aligned homeotropically and the film gets the optical properties of a positive C crystal plate (Figure 7b). At much higher intensities of UV light ($I \geq 30$ mW/cm²) both in-plane and out-of-plane retardations tend to 0 at saturation, which corresponds to an isotropic order (Figure 7c).

ATR results for P8 films are given in Table 3. They correspond to the case of strong irradiation, which leads to isotropy after irradiation. Surprisingly, under irradiation P8 film

TABLE 3: ATR Results for P8 Films Corresponding to 365 and 457 nm Irradiation

film	film history	film params					film struct
		$d, \mu\text{m}$	n_x	n_y	n_z	$\langle n \rangle$	
Irradiation with $\lambda = 365$ nm (x Polarization, 30 mW/cm ²)							
P8-1	before irradiatn	1.448	1.569	1.574	1.540	1.561	negative C film
	under irradiatn, 30 min	1.441	1.549	1.560	1.547	1.554	positive A film
	relaxatn, 15 min	1.452	1.550	1.553	1.549	1.551	isotropic film
	relaxatn, 5 h	1.460	1.558	1.560	1.558	1.559	isotropic film
	after 2nd irradiatn: 457 nm (x polarizatn), 40 min	1.457	1.525	1.655	1.525	1.568	positive A film
Irradiation with $\lambda = 457$ nm (x Polarization, 100 mW/cm ²)							
P8-2	before irradiatn	1.408	1.555	1.621	1.517	1.564	biaxial film
	irradiatn 60 min	1.417	1.525	1.637	1.533	1.565	positive A film
	relaxatn 20 min	1.404	1.534	1.650	1.533	1.573	positive A film

TABLE 4: ATR Results for P9 Films Corresponding to 365 and 457 nm Irradiation

film	film history	film params					film struct
		$d, \mu\text{m}$	n_x	n_y	n_z	$\langle n \rangle$	
Irradiation with $\lambda = 365$ nm (x Polarization, 50 mW/cm ²)							
P9-1	before irradiatn	2.879	1.556	1.563	1.561	1.560	isotropic film
	under irradiatn, 30 min	2.967	1.538	1.539	1.540	1.539	isotropic film
	relaxatn, 10 min	2.953	1.548	1.550	1.545	1.548	isotropic film
Irradiation with $\lambda = 457$ nm (x Polarization, 100 mW/cm ²)							
P9-2	before irradiatn	1.735	1.543	1.557	1.554	1.551	slightly biaxial film
	under irradiatn, 40 min	1.746	1.538	1.553	1.551	1.547	negative A film
Irradiation with Unpolarized $\lambda = 365$ nm Followed by x Polarized $\lambda = 457$ nm							
P9-2	$\lambda = 365$ nm, 20 min, relaxatn, 5 min	1.764	1.537	1.547	1.538	1.540	isotropic film
	$\lambda = 457$ nm, 30 min, relaxatn 5 min	1.722	1.512	1.560	1.573	1.550	negative A film

demonstrates weak in-plane positive order. It may be caused by a hole-burning process, which dominates in this case, because of the high excitation rate of trans and of the relatively long lifetime of cis isomers. After irradiation is cut off, the induced order relaxes, presumably because of enhanced rotational diffusion of azochromophores in the “melted” polymer film. Polymer P8 demonstrates also some other strange properties. It is the only homologue exhibiting an in-plane alignment in the initial state and an out-of-plane preference after a soft UV irradiation. This implies that in-plane alignment in P8 is metastable, in big contrast to P1–P7 homologues where in-plane alignment is very stable. One more distinguishing feature, according to both TNE and ATR results, the symmetry of the exciting light influences the angular distribution of azochromophores in P8 only for very small irradiation doses or under irradiation.

For polymer P9, the values of $(n_y - n_x)d$ and $(n_z - n_x)d$ at various irradiation times are plotted in Figure 8c. Both in-plane and out-of-plane retardation curves go through a maximum and converge to zero for long-time irradiation. This implies isotropic orientation in the saturation state (Figure 7c), which can be obtained by strong depletion of trans chromophores. Compared with P8, the isotropic state in P9 polymer is reached for lower intensities of the exciting light. This could be caused by the longer lifetime of cis isomers (and other unknown photoproducts) and, consequently, by a stronger depletion of trans isomers. This almost irreversible excitation cannot induce effective angular redistribution. ATR results (Table 4) confirm the isotropic state of P9 after irradiation but also under irradiation.

As mentioned before, since the number of trans isomers permanently changes with the irradiation dose, the total absorption method cannot be applied to estimate order parameters of azochromophores in P8 and P9 films.

Finally, it is worthy to discuss relaxation peculiarities of the induced order. In P1–P7 homologues the induced order is very stable and persists over many months of our observation. The order induced in P8 and P9 films partially relaxes with the

characteristic time comparable with the lifetime of photoproducts. However, it also contains a long-living component (months of living), which might be assigned to photoreorientation and accompanied photoselection based on irreversible photochemistry.

2. *Irradiation with Polarized Visible Light ($\lambda_{ex2} = 457$ nm or $\lambda_{ex3} = 488$ nm).* The values of the in-plane $(n_y - n_x)d$ and the out-of-plane $(n_z - n_x)d$ retardation for polymer P1, corresponding to various exposure times with $\lambda_{ex3} = 488$ nm excitation (x -polarization), are presented in Figure 11a. The observed behavior is similar to the case of 365 nm irradiation; on the first irradiation stage, a biaxial orientation is induced, whereas the saturation state is characterized by an uniaxial in-plane alignment, as depicted in Figure 7e.

In parallel with TNE studies, the measurement of D_x and D_y absorption components have been performed. The D_z component has been estimated by the total absorption method (by setting $D_z = D_x$ at saturation of the excitation). D_x , D_y , and D_z versus the irradiation dose are presented in Figure 12a. These data can be used to calculate order parameter components for each irradiation step, as it was done in case of $\lambda_{ex1} = 365$ nm irradiation. Before irradiation one has $S \equiv S_{zz} = -2S_{xx} = -2S_{yy} = -0.1$. For the saturation state, one obtains $S \equiv S_{yy} = -2S_{xx} = -2S_{zz} = 0.56$. ATR results (Table 2) are in full agreement with the results of TNE and absorption measurements. In addition, they show that, under irradiation, independently of the intensity of excitation, the order of a positive A plate clearly appears, in contrast to the case of $\lambda_{ex1} = 365$ nm irradiation.

The results for P2–P7 are similar to those for P1. The difference is only in the value of the order parameter, $S \equiv S_{yy}$, reached at saturation. The dependence of S on the number m of CH₂ groups in the main-chain spacer is shown in Figure 10 (curve 2). For all homologues, the order induced by $\lambda_{ex3} = 488$ nm irradiation is higher than that induced by $\lambda_{ex1} = 365$ nm. This may be explained by substantially lower concentration of nonmesogenic cis isomers at $\lambda_{ex3} = 488$ nm destroying the orientational order, as discussed above. Other mechanisms, not

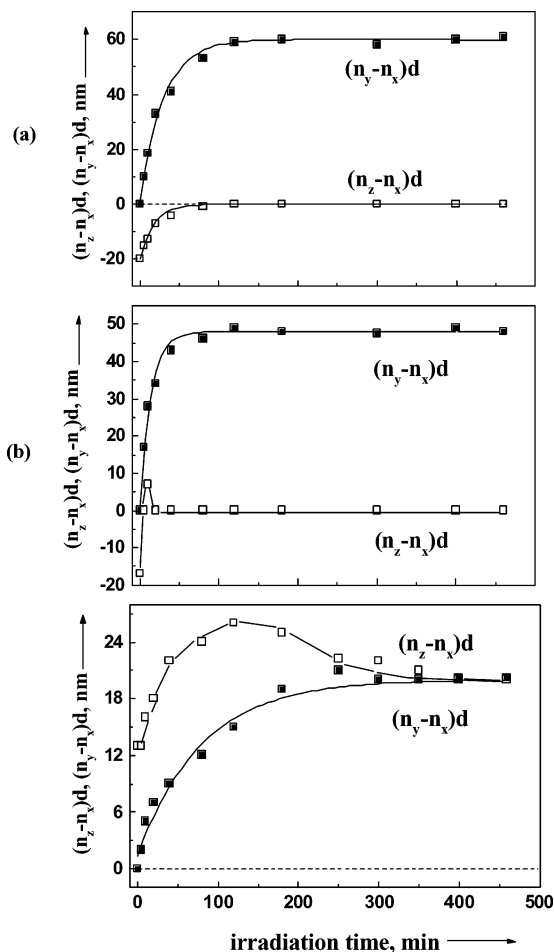


Figure 11. Birefringence kinetics for polymers (a) P1, (b) P8, and (c) P9 for successive exposure doses. Irradiation is with $\lambda_{\text{ex}3} = 488$ nm ($I = 750$ mW/cm², x polarization).

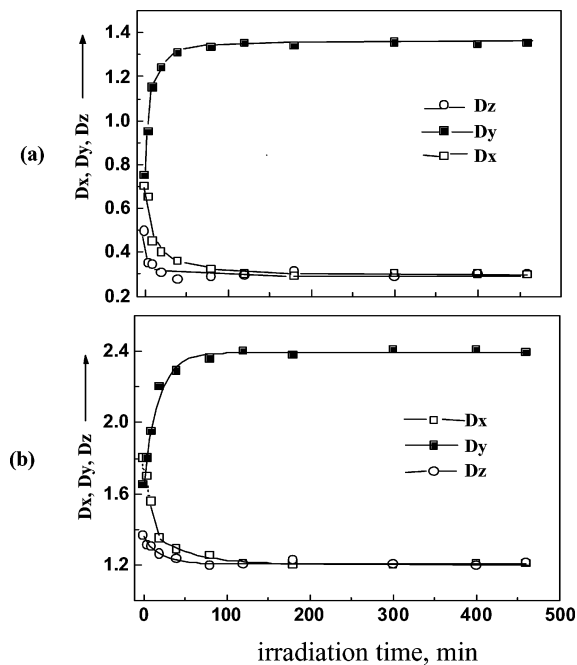


Figure 12. Experimentally measured (D_x , D_y) and calculated (D_z) kinetics for polymers (a) P1 and (b) P8. Irradiation conditions are the same as in Figure 11.

specific for LC polymers, can also contribute to the better ordering by 488 or 457 nm excitation, such as better penetration of pumping light in the film, because of low $n\pi^*$ absorption of

chromophores, as compared with $\pi\pi^*$ absorption, and intensification of reorientation due to a faster trans–cis–trans cycling caused by enhanced excitation probability of cis form in the $n\pi^*$ spectral range.^{18,20}

Figure 11b shows the $(n_y - n_x)d$ and $(n_z - n_x)d$ versus exposure time curves for P8. The nonstability of $(n_z - n_x)d$ values in the very beginning stage of irradiation may reflect metastable character of the in plane alignment in a nonirradiated film. Rapidly the film becomes uniaxial (structure of positive A plate, Figure 7e), like P1. This is confirmed by ATR experiments (Table 3), as well under irradiation as after relaxation in dark. The behavior is completely different from that obtained with 365 nm excitation. Like with P1–P7, one can interpret the results related to 488 and 457 nm irradiation of P8 on the basis of the low excitation rate of trans and a high excitation rate of cis isomers, which results in small concentration of cis and intensive trans–cis–trans cycling that results in a fast reorientation of trans isomers.

As discussed in subsection III.A.2, in case of P8, a small concentration of cis form at $\lambda_{\text{ex}3} = 488$ nm excitation allows us to apply the method of total absorption. As polymer films exhibit in-plane uniaxial order at the saturation of irradiation, $D_z = D_x$ in this state. The calculated $D_z(t)$ curve, along with $D_x(t)$ and $D_y(t)$ curves, is shown in Figure 12b. These results give the same symmetry before irradiation as the refractive index measurements ($D_z < D_x \approx D_y$). There is one more proof of the validity of total absorption approach for this experimental case. At saturation, $S \equiv S_{yy} = -2S_{xx} = -2S_{zz} = 0.25$.

Figure 11c shows TNE results for a P9 film. Up to 300 min of irradiation the film remains biaxial, and finally, at saturation, the order becomes uniaxial, with a random distribution of azochromophores in the plane perpendicular to E_{ex} (oblate order optically equal to the negative A film, Figure 7f). The latter result is confirmed by ATR measurements (Table 4). It suggests that, at saturation, the distribution of chromophores totally conforms to the light symmetry (LC self-ordering is suppressed). This behavior was earlier described for amorphous azopolymers¹⁰ and for some LC azopolymer on methacrylate base.²⁴

Since P9 film demonstrates considerable nonreversible spectral changes under $\lambda_{\text{ex}3} = 488$ nm irradiation, estimation of the D_z component by the total absorption method is not possible. For this case, similarly to the case of $\lambda_{\text{ex}1} = 365$ nm irradiation, new approaches for the estimation of S_{ii} ($i = x, y, z$) components are required. One of them is considered in our recent publication.²⁴ It is based on the calculation of the order parameter components in the frame of the theoretical model of 3D photoorientation on the basis of the data of in-plane absorption and photochemical constants experimentally measured. Another approach consists of the monitoring of 3D absorption using the multiple beam technique described in ref 43.

In the end, the order induced by $\lambda_{\text{ex}2} = 457$ nm or $\lambda_{\text{ex}3} = 488$ nm is extremely stable in all polymers; it practically does not show relaxation over several months of our monitoring. This confirms the effective photoreorientation mechanism of PIA in homologues P1–P8 and, possibly, in P9, in which stable order may be also caused by photoselection on the basis of nonreversible photochemistry.

3. Subsequent Irradiation with Several Excitation Lines. In the nonirradiated films the azochromophores are mainly in trans configuration. The concentration of cis isomers can be substantially increased in polymers P8 and P9 by irradiation with 365 nm light which lies in the absorption band of trans azochromophores. In a new experiment, films of P1, P8, and P9 were preirradiated with nonpolarized UV light, $\lambda_{\text{ex}1} = 365$ nm, $I =$

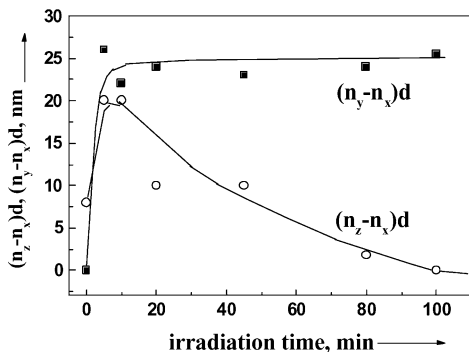


Figure 13. Birefringence kinetics for preirradiated film of polymer P8. The film is preirradiated with nonpolarized UV light ($\lambda_{\text{ex1}} = 365$ nm, $I = 20$ mW/cm², 30 min) and, subsequently, stepwise irradiated with polarized visible light ($\lambda_{\text{ex3}} = 488$ nm, $I = 750$ mW/cm²).

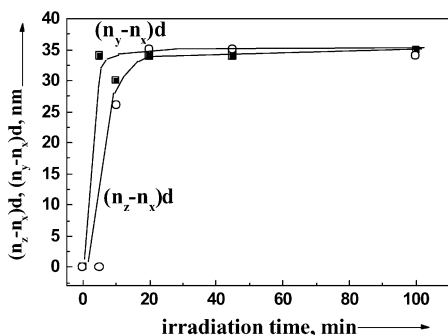


Figure 14. Birefringence kinetics for preirradiated film of polymer P9. Irradiation conditions are the same as in Figure 13.

25 mW/cm², during 30 min. Immediately after this irradiation, films were stepwise irradiated with polarized light, $\lambda_{\text{ex3}} = 488$ nm, and the corresponding 3D order was studied by TNE. In P1, the UV preirradiation has no influence on the dynamics of the 3D order induced by 488 nm light. This is not surprising, since the relaxation of cis isomers is very fast. The situation is different for P8 and P9 polymers, as shown, correspondingly, in Figures 13 and 14. In both cases, the type of 3D orientation at saturation is the same as without preirradiation (structure of positive A plate for P8 and structure of negative A plate for P9). This is also confirmed by ATR results (see Tables 3 and 4). However, the reorientation dynamics is different in preirradiated and nonpreirradiated films.

In P9 film, the saturation state (negative oblate order with x symmetry axis, Figure 7f) is reached considerably faster than in the nonpreirradiated film. One also sees that $n_z - n_x$ monotonically reaches its asymptotic value without the first maximum observed with only 488 nm irradiation. With UV preirradiation, the trans state is strongly isotropically depleted and the population of the cis state is large (see Figure 6). Then the photostationary state is reached very fast in the subsequent 488 nm irradiation, because of high excitation probability of cis isomers.

On the first irradiation stage (10 min, Figure 13), the preirradiated P8 film exhibits the same oblate order as P9, but in the following stage, the out-of-plane retardation slowly falls to zero and, in the saturation state, the prolate order with the y ordering axis is formed (see Figure 7e).

The reverse sequence of irradiation, when films are first irradiated with polarized $\lambda_{\text{ex3}} = 488$ nm light and then with $\lambda_{\text{ex1}} = 365$ nm nonpolarized light, has also been studied. The resultant orientation strongly depends on the UV irradiation intensity. In case of low intensity ($I < 5$ mW/cm²) the order induced with $\lambda_{\text{ex3}} = 488$ nm persists in all polymers, except P9

in which the order is substantially destroyed by UV action. The UV light of higher intensity ($I > 20$ mW/cm²) practically erases the order preliminarily induced.

IV. Conclusions

Thus, 3D consideration of the photoinduced order in azopolymers reveals new ordering features, which cannot be observed with 2D studies. First what can be concluded is that even nonirradiated films may possess spatial anisotropy, because of preferential in-plane or out-of-plane orientation of azochromophores.

The second conclusion is that the 3D order realized under irradiation can be far away from the order required by light symmetry. In the usual case of amorphous polymers (like PMMA-DR1¹⁰) polarized light irradiation induces random orientation of azochromophores in the plane perpendicular to light polarization E_{ex} (oblate order with the symmetry axis along E_{ex}). In the case of our LC polymers, this type of orientation is realized only in polymer P9 containing azochromophores tailed with long alkyl fragments. The photoinduced orientation in P1–P7 polymer films is more similar to that in the planar layers of low-molecular-weight LC: azochromophores are uniaxially aligned “in-plane” with the ordering axis perpendicular to E_{ex} . This suggests that photoirradiation, through the enhancement of the molecular mobility, activates processes of spontaneous ordering intrinsic for the liquid crystalline compounds. The latter processes substantially modify orientational order determined by the symmetry of the exciting light. The liquid crystal self-organization is so pronounced due to the low melting temperatures of the studied polyesters.

The results presented in this paper show that the spontaneous order and the photoinduced order strongly depend on the structure of chromophores, as well as on that of the main polymer chain. The molecular structure determines the photoorientation properties of azochromophores by modifying their photochemical properties and intrinsic self-organization.

In the following we list some conclusions related to the influence of the molecular structure on the 3D alignment of azochromophores in nonirradiated and irradiated films:

(1) In the P0–P7 series, the lengthening of the alkyl main-chain spacer leads to transition from the out-of-plane, in P0, to the in-plane orientation, in P1–P7 homologues.

(2) The change of the tail substitute in azochromophore in the sequence NO₂ (P1) → OCH₃ (P8) → OC₄H₉ (P9) enhances preference to the out-of-plane orientation. It also reduces the self-ordering strength, as well in nonirradiated films as in the photooriented ones. The lifetime of the cis isomer also grows in this sequence. In contrast to other homologues, the photochemistry of P9 is not well understood and appears to involve photochemical effects more complicated than trans–cis photoisomerization.

(3) The photoinduced order, corresponding to the saturation of irradiation, is uniaxial (except in the case of isotropic orientation). It is determined by the symmetry of light and by the self-ordering of mesogenic compounds. The photoinduced order strongly depends on the photoordering mechanisms, which, in turn, are determined by the spectral composition of light, as described below.

(4) Irradiation with $\lambda_{\text{ex1}} = 365$ nm, which corresponds to an effective absorption within the $\pi\pi^*$ band of azochromophores, leads to a positive (prolate) in-plane order, with the ordering axis perpendicular to E_{ex} , in P1–P7 polymers (case of fast cis to trans relaxation), but to homeotropic or isotropic orientation in P8 and to isotropic orientation in P9. The isotropic orientation

is caused by high concentration of cis isomers with a long lifetime in P8 and still longer in P9.

(5) Irradiation with $\lambda_{\text{ex}2} = 457$ nm and $\lambda_{\text{ex}3} = 488$ nm, corresponding to $n\pi^*$ absorption band of azochromophores (effective absorption of cis isomers), results in a positive in plane ordering in P1–P7 as well as in P8 homologue. A negative (oblate) order with the symmetry axis along E_{ex} is observed in polymer P9.

(6) The photoinduced ordering is not observed in P0, probably because of the strong aggregation of azochromophores.

The regularities we observed for the studied series of polyesters are in good agreement with the regularities earlier observed for methacrylate-based azopolymer^{23,24} as well as for the polymers with photosensitive cinnamoyl groups undergoing (2 + 2)-cycloaddition reaction under irradiation.³¹ So the regularities established may be the general rules, which can be used to predict orientational order in other types of polymers. As we believe, the obtained empirical rules may simplify the optimization of anisotropic polymer films for new applications, for instance, retardation films for LCD⁴⁴ or photoaligning layers for liquid crystal cells.^{45,46}

It is important to note that in the present studies we cut off the film thickness range less than 500 nm. However, according to our late results, the 3D order in thin films ($d < 200$ nm) may be totally different from that in the thick films presently studied. This difference might be caused by self-assembling at the interfaces as a quite important self-organization factor.

We continue to improve the understanding of photoordering processes in LC azopolymers. Soon the LC polymers described in this paper will be additionally tested with a 3D absorption technique recently developed.⁴³

Acknowledgment. The studies were supported by a personal NATO grant (OTAN-France) for O.V.Y. The authors thank Rolland Hierle for the help in calorimetric studies and Isabelle Ledoux-Rak for fruitful discussions.

References and Notes

- Weigert, F.; Verh. *Phys. Ges.* **1919**, *21*, 485; *Z. Phys.* **1921**, *5*, 410.
- Sekkat, Z.; Dumont, M. *Appl. Phys. B* **1992**, *54*, 486; *Nonlinear Opt.* **1992**, *2*, 359.
- Charra, F.; Kajzar, F.; Nunzi, J. M.; Raimond, P.; Idiart, E. *Opt. Lett.* **1993**, *18*, 941.
- Fiorini, C.; Charra, F.; Nunzi, J. M.; Raimond, P. *Nonlinear Opt.* **1995**, *9*, 339–346.
- Brasselet, S.; Zyss, J. *Opt. Lett.* **1997**, *19*, 1464; *J. Opt. Soc. Am. B* **1998**, *15*, 257–288.
- Neporent, B. S.; Stolbova, O. V. *Sov. Opt. Spektrosk.* **1961**, *10*, 287; *Opt. Spektrosk.* **1963**, *14*, 624.
- Makushenko, A.; Neporent, B.; Stolbova, O. *Sov. Opt. Spektrosk.* **1971**, *31*, 741.
- Eich, M.; Wendorff, J. H.; Reck, B.; Ringsdorf, H. *Macromol. Chem., Rapid Commun.* **1987**, *8*, 59–63.
- Hvilsted, S.; Andruzzi, F.; Ramanujam, P. S. *Opt. Lett.* **1992**, *17*, 1234–1236.
- Dumont, M.; Sekkat, Z. *Proc. SPIE* **1992**, *1774*, 188–199.
- Natansohn, A.; Rochon, P.; Gosselin, J.; Xie, S. *Macromolecules* **1992**, *25*, 2268–2273.
- Wiesner, U.; Reynolds, N.; Boeffel, Ch.; Spiess, H. W. *Liq. Cryst.* **1992**, *11*, 251–267.
- Petri, A.; Kummer, S.; Breuchle, C. *Liq. Cryst.* **1995**, *19*, 277–287.

- Puchkovskaya, G.; Reshetnyak, V.; Tereshchenko, A.; Yaroshchuk, O.; Lindau, J. *Mol. Cryst. Liq. Cryst.* **1998**, *321*, 31–43.
- Rochon, P.; Batalla, E.; Natansohn, A. *Appl. Phys. Lett.* **1995**, *66*, 136–138.
- Jiang, X. L.; Li, L.; Kumar, J.; Kim, D. Y.; Shivshankar, V.; Tripathy, S. K. *Appl. Phys. Lett.* **1996**, *68*, 2618–2620.
- Lefin, P.; Fiorini, C.; Nunzi, J. M. *Opt. Mater.* **1998**, *9*, 323–328.
- Sekkat, Z.; Dumont, M. *Synth. Met.* **1993**, *54*, 373–381.
- Dumont, M.; Hosotte, S.; Froc, G.; Sekkat, Z. *Proc. SPIE* **1993**, *2042*, 2–13.
- Dumont, M.; Osman, A. El. *Chem. Phys.* **1999**, *245*, 437–462.
- Dumont, M. *Nonlinear Opt.* **2000**, *25*, 195–199.
- Kiselev, A.; Yaroshchuk, O.; Zakrevskyy, Yu.; Tereshchenko, O. *Condens. Matter Phys.* **2001**, *4*, 67–75.
- Yaroshchuk, O.; Kiselev, A.; Zakrevskyy, Yu.; Stumpe, J.; Lindau, J. *Eur. Phys. J., E* **2001**, *6*, 57–67.
- Yaroshchuk, O.; Kiselev, A.; Zakrevskyy, Yu.; Bidna, T.; Chien, L.-C.; Lindau, J. *Phys. Rev. E* **2003**, *68*, 011803–011818.
- Fischer, M.; Osman, A.; Blanche, P.; Dumont, M. *Synth. Met.* **2000**, *115*, 139–144.
- Phaadt, M.; Boeffel, Ch.; Spiess, H. W. *Acta Polym.* **1996**, *47*, 35–39.
- Page, R. H.; Julrich, M. C.; Reck, B.; Sen, A.; Twieg, R. J.; Swalen, J. D.; Bjorklund, G. C.; Willson, C. G. *J. Opt. Soc. Am. B* **1990**, *7*, 1239–1244.
- Dumont, M.; Levy, Y.; Morichere, D. Electrooptic organic waveguides: optical characterisation. In *Organic molecules for Nonlinear optics and photonics*; Proceedings of ARW, La Rochelle, France, 1991; NATO ASI Series; Messier, J., Kajzar, F., Prasad, P., Eds.; Kluwer Acad. Publ.: Dordrecht, The Netherlands, 1991; E194, pp 461–480.
- Yaroshchuk, O.; Sergan, T.; Lindau, J.; Lee, S. N.; Kelly, J.; Chien, L.-C. *J. Chem. Phys.* **2001**, *114* (12), 5330–5337.
- Yaroshchuk, O.; Sergan, T.; Lindau, J.; Lee, S. N.; Kelly, J.; Chien, L. C. *Mol. Cryst. Liq. Cryst.* **2001**, *359*, 301–313.
- Yaroshchuk, O.; Sergan, T.; Gerus, I. *Jpn. J. Appl. Phys.* **2002**, *41*, 275–379.
- Kulinna, C.; Hvilsted, S.; Hendann, C.; Siesler, H.; Ramanujam, P. S. *Macromolecules* **1998**, *31*, 2141–2151.
- Brown, D.; Natansohn, A.; Rochon, P. *Macromolecules* **1995**, *28*, 6116–6123.
- Wu, Y.; Zhang, Q.; Kanazava, A.; Shiono, T.; Ikeda, T.; Nagase, Y. *Macromolecules* **1999**, *32*, 3951–3956.
- Böhme, A.; Novotna, E.; Kresse, H.; Kuschel, F.; Lindau, J. *Macromol. Chem.* **1993**, *194*, 3341–3344.
- Ober, Ch. K.; Jin, J.-I.; Lenz, R. W. Liquid Crystal Polymers with Flexible Spacers in the Main Chain. *Adv. Polym. Sci.* **1984**, *59*, 111.
- Yaroshchuk, O.; Tereshchenko, A.; Zakrevskyy, Yu.; Shansky, I. *Mol. Cryst. Liq. Cryst.* **2001**, *361*, 187–192.
- Yaroshchuk, O.; Dumont, M.; Lindau, Ju.; Bidna, T. Photoinduced 3D Orientational Order in Liquid Crystalline Azopolymers Studied by the Method of Attenuated Total Reflection. *Mol. Cryst. Liq. Cryst.*, in press.
- Kasha, M.; Rawls, H. R.; Boyoumi, M. A. *Pure Appl. Chem.* **1965**, *11*, 371–392.
- An introduction to ultrathin organic films. From Langmuir–Blodgett to self-assembly*; Ulman, A., Ed.; Academic Press: New York, 1991.
- Kanazawa, A.; Hirano, S.; Shido, A.; Hasegawa, M.; Tsutsumi, O.; Shiono, T.; Ikeda, T.; Nagase, Yu.; Ikiyama, E.; Takamura, Y. *Liq. Cryst.* **1997**, *23*, 293–298.
- Komitov, L.; Yamamoto, J.; Yokoyama, H. *J. Appl. Phys.* **2001**, *89* (12), 7730.
- Nguyen, N.; Kim, Thi; Dumont, M. 3D characterization of molecular photoorientation: application to all-optical poling. In *Organic Nanophotonics*; Charra, F., et al., Eds.; Kluwer Academic Publisher: Dordrecht, The Netherlands, 2003; pp 395–404.
- Yaroshchuk, O.; Reznikov, Yu.; Sergan, T.; Kelly, J.; Chien, L.-C. Pending U.S. Patent 09/722,991, 2001.
- Gibbons, W. M.; Kosa, T.; Palffy-Muhoray, P.; Shannon, P. J.; Sun, S. T. *Nature* **1995**, *377* (7), 43–46.
- Zakrevskyy, Yu.; Yaroshchuk, O.; Kelly, J.; Chien, L.-C.; Lindau, J. *Mol. Cryst. Liq. Cryst.* **2002**, *375*, 769–783.